



SYNTHESIS OF CELLULOSE ACETATE NANOFIBER (CANF) FROM BACTERIAL CELLULOSE (BC) INCUBATED FROM CANNERY SEAFOOD WASTEWATER (CSW) USING ACETOBACTER XYLINUM

Sunun Khami¹, Wipawee Khamwichit¹ and Kowit Suwannahong²

¹Civil and Environmental Engineering, Walailak University, Thai Buri, Tha Sala District, Nakhon Sri Thammarat Province, Thailand

²Public Health, Western University, Kanchanaburi Campus, Salongrue, Heuykrachao District, Kanchanaburi Province, Thailand

E-Mail: sea.khasee@gmail.com

ABSTRACT

There are increasing demands to substitute plastic produced from the petrochemical industry with bacterial cellulose which were produced from microorganisms as *Acetobacter xylinum* strain, a gram negative bacterium. *A.xylinum* metabolizes carbon source in cannery seafood wastewater (CSW) and converts it into bacterial cellulose (BC) which has unique properties including high purity, crystallinity and mechanical strength. These properties are induced by the main components of BC with are cellulose and hemicellulose. The aim of this study was to produce bacterial cellulose from CSW collected from factories in the southern areas of Thailand. The CSW was used as a carbon source for the growth of bacteria. The best conditions for cultivation to obtain the maximum yield (1.14 g) and COD treatment (71.2 %) were carbon source (COD ratio) 11, 971 mg/L, 5 ml of *A.xylinum* added, cultivation temperature and time of 40 °C and 21 days. BC synthesized from CSW was then undergone though semi-acetylation process to produce cellulose acetate nanofiber (CANF). CANF exhibits desirable mechanical properties, including high tensile strength (90.71 MPa), and young modulus (439.36 MPa) due to its uniform and ultrafine fibrous network structure. It can be sterilized without any changes to its structure and properties. The morphology properties of SEM images of CANF synthesized in the study was approximately 30-100 nm. The physical properties of CANF were studied with ATR-FTIR spectroscopy which shown adsorption spectrum at 3343 cm⁻¹, 2898 cm⁻¹, 1458 cm⁻¹, 1427 cm⁻¹, 1158 cm⁻¹ and 1028 cm⁻¹ which correspond to O-H stretching, C-H stretching, C-H bending, CH₂ bending, C-O-C stretching and C-O stretching, respectively. Thermal analysis showed a DTG peak at 430°C, which falls in the range of cellulose degradation peaks (380°C-460°C). The peak confirms that cellulose was the major component of CANF. Thus, the main component of CANF were cellulose and hemicellulose. The synthesized CANF can be used as membrane media and also has its chemical properties like petroleum polymer. Results suggested that the similar property can be observed when compared with petroleum plastic, however with the exception of methyl group (CH₃). Methyl group which can be found in plastic synthesized from petrochemical is responsible for the strength of plastic. Thus, CANF, synthesized in this study, is not as strong as petrochemical plastic. But it can be used to produce bio-plastics because of the -CH and -CH₂ functional group attached. With the similar physical and chemical properties to those of petrochemical plastic, CANF can be used as biopolymer.

Keywords: bacterial cellulose (BC), acetobacter xylinum, cannery seafood wastewater (CSW), cellulose acetate nanofibers (CANF), semi-acetylation.

1. INTRODUCTION

Petro chemical is used primarily in the production of plastic, however production process induces both wastewater and air pollution [1]. Aside from that impact, manufacture of plastic in Thailand requires imported raw material which pushes up its production cost. Therefore study about an alternative raw material to produce bioplastic has drawn an attention from environmental process researchers. It initially provides an alternative process which is less expensive and more environmental friendly. Especially raw materials from water waste of canned seafood industry ranges from 30,000 to 50,000 L/day. Since CSW was high BOD₅ (100-3,000 mg/L), COD (1,000-18,000 mg/L), and nitrogen content (80-1,000 mg/L) [2], this study used CSW to be carbon source in the cultivation process of BC synthesis. *A.xylinum* can grow and form BC [3]; as a result treatment of COD and BOD as well as foul odors can be achieved.

Set of experiment were designed using response surface modeling (RSM). RSM is an empirical statistical technique that uses quantitative data obtained from

appropriately designed experiments to determine regression model and operating conditions [4, 5, 6, 7, 8]. It can also be used to design factorial experiments, in order to build mathematical models which allow one to assess the effects of several factors onto a desired response. It is suitable for multi-factor experiments and searches the common relationship between various factors for the most favorable conditions of the processes. The examination dosage of a combined effect of various process parameters like carbon Source (COD ratio), *A.xylinum* and temperature was performed using Box-Behnken model experimental design in RSM. The aim of this research was to determine the optimum condition of BC and CANF synthesis process.

2. MATERIALS AND METHODS

2.1 Cultivation of bacterial cellulose (BC)

The studied conditions for cultivation of bacteria cellulose from cannery seafood wastewater (CSW) in this study included; carbon source (COD ratio), *A.xylinum*



dosage, and temperature. Initial concentration in this study was 4% Brix, *A.xylinum* was cultured on Num-tan-wan (sucrose) agar at 30 °C for 7 days to produce starter culture [9, 10]. *A.xylinum* dosages used in the cultivation were 1, 3, and 5 mL/1,000 mL of CSW, the carbon source (COD ratio) were 5, 997, 8, 996 and 11, 971 mg/L, and incubating temperatures were 20, 30 and 40 °C. Fifteen sets of experiment were performed under these various conditions. The steps of cultivation were as followed. First, 1000 mL of CSW was filtrated using filtration glass set (Rocker model VF7 cat.167200-07). Second, the filtrate was heated in autoclave (HUMANLAB model DAC-45/45L) at 121°C for 15 minutes, then it was taken off and cooled down to ambient temperature. *A.xylinum* was added into the filtrate with the ratio as described previously. Next, the solution was cultivated in incubator (Binder model BD115) at 20, 30 and 40°C for 21days. The bacterial cellulose was formed as shown in Figure-1. BC was undergone through semi-acetylation process to form CANF. To do so, BC was set at room temperature for 3 days, after that it was boiled with 2% NaOH to at 60 °C for 2 hrs to rip out of bacterial cell debris. Next, the BC solution was boiled with 40 mL of 75% ethanol at 60 °C for 3 hrs. Later, it was dried in an oven at 60 °C for 3 hrs. Dried BC was blended with mixture of 40 mL of acetic acid, 50 mL of toluene, and 0.2 mL of 60% perchloric acid. BC was washed with 40 mL 75% ethanol for around 2 hrs. Finally, BC sample (maintaining its original appearance) was thoroughly washed with distilled water to remove byproducts, remaining reagents and put in oven for 3 hrs at 60 °C to obtain CANF as shown in Figure-2.

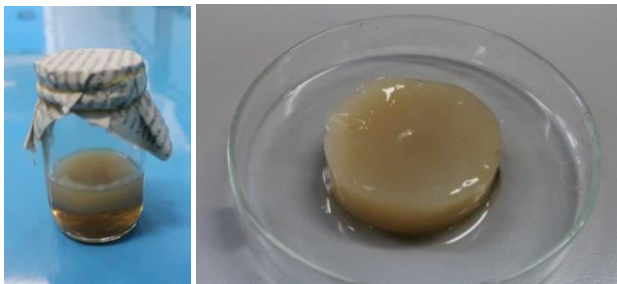


Figure-1. Bacterial cellulose after 21 day.



Figure-2. Cellulose acetate nanofibers synthesized from BC.

2.2. Response surface methodology (RSM)

The three-level Box-Behnken experimental design with categorical factor were employed to optimize the yield capacity of the bacterial cellulose (BC) and treatment of cannery seafood wastewater. The design was composed of three levels (low, medium and high) and a total of 15 runs were carried out to optimize the chosen variables; carbon source (COD ratio), *A.xylinum* dosage, and temperature. For the purpose of statistical computations, the three independent variables were denoted as x_1 , x_2 , and x_3 , respectively. According to the preliminary experiments, the range and levels used in the experiments are selected and listed in Table-1. The main effects and interactions between factors were determined. The experimental design matrix by the Box-Behnken design is tabulated in Table-2. For RSM, the most commonly used second-order polynomial equation developed to fit the experimental data and determine the relevant model terms can be written as:

$$Y = \beta_0 + \beta_1x_1 + \beta_2x_2 + \beta_{11}x_1^2 + \beta_{22}x_2^2 + \beta_{12}x_1x_2 + \varepsilon \quad (1)$$

where Y represents the predicted response, i.e. the yield (g) and capacity of COD wastewater treatment, β_0 , the constant coefficient, β_1 and β_2 , the linear coefficient of the input factor x_1, x_2, x_{11}, x_{22} , and β_{12} the quadratic coefficient of the input factors x_{11}, x_{22} , β_{11} and β_{22} , the different interaction coefficients between input factors x_1, x_2 and ε , the error of the model [11]. The equation expresses the relationship between the predicted response and independent variables in coded values according to Table-1.

Table-1. Factors and levels used in the experiment design.

| Range of parameters | Values |
|---------------------------------|----------------------|
| Carbon Source (COD ratio), mg/L | 5,997, 8,996, 11,971 |
| <i>Acetobacter Xylinum</i> , mL | 1, 3, 5 |
| Temperature °C | 20, 30, 40 |
| Operating conditions | Values |
| Reaction time, day | 21 |

3. CHEMICAL AND PHYSICAL ANALYSIS

3.1 Morphology properties

The microstructure of the bacterial cellulose will be examined by using the Scanning Electron Microscope (SEM, Model Jx A-840, JEOL) [12]. BC was dried in hot air oven (BINDER model FD115) at 65°C for 6 hours. After 6 hours, it was taken off from oven and put in desiccator (Eureka model RT-48C) until it cooled to ambient temperature. The dry BC will be mounted on aluminum stubs, sputter-coated with gold and examined in a Jx A-840 scanning electron microscope. The images from the scanning electron microscope will be analyzed



with Micosun 2000/s image analysis software to obtain data on the distribution of particles and fibers obtained in the nanofiber [13]. This image analysis will be conducted at magnifications of 20,000X.

3.2 Tensile stress

Tensile stress of bacterial cellulose was tested using tensile stress machine (Shimadzu model DSS-10T). Analysis procedure was followed ASTM D638 standard, in which sample with thickness of 7.5 mm. and width of 25.4 mm. was placed in the clamps. Tensile force was increased until sample was torn. Three replications were done [9].

3.3 FTIR spectra analysis

Functional group of chemical structure of dry bacterial cellulose was analyzed by ATR Fourier Transform Infrared Spectrometer (Perkin Elmer model Spectrum One) using attenuated total multiple reflection method (ATR-FTIR) technique [9]. Spectrum used in the study was 650 - 4000 cm^{-1} .

3.4 Glass transition temperature (T_g)

The sample will be dried as described previously, and then the change of the thermal property will be estimated by Differential Scanning Calorimetry (DSC) (Netzsch model 204 F1 Phoenix). The analysis will be proceeded as instructed by the ASTM D792 standard. Weight of the sample used in the analysis is 1 gram and its surface is 1 cm x 1 cm [9]. Three replications will be done.

4. RESULTS AND DISCUSSIONS

4.1 Metabolic pathway of cellulose-producing bacteria

The most commonly studied model bacterium for the production of BC is *A.xylinum* due to its ability to produce cellulose from a wide range of carbon sources. The *Acetobacter* strains are gram-negative, aerobic, and exist as straight, slightly bent rods or ellipsoidal in the range of 0.6 μm x 4 μm .

Cellulose-producing bacteria, such as *A.xylinum*, operates in the pentose-phosphate cycle or the Krebs cycle, depending on the physiological state of the cell coupled with gluconeogenesis [12]. The pentose-phosphate cycle involves the oxidation of carbohydrates and the Krebs cycle involves the oxidation of acetate-derived carbohydrates, fat, and proteins, such as oxalosuccinate and α -ketoglutarate. However, *A.xylinum* is not able to metabolize glucose anaerobically because it lacks phosphofructose kinase, which is required for glycolysis [9]. Biosynthesis of cellulose by *A.xylinum* have been studied and reported by numerous researchers [9, 12].

CSW is used by *A.xylinum* as carbon source for the cellulose production. The high performance liquid chromatography analysis (HPLC) showed the concentration of sucrose, glucose, fructose, acetic acid and lactic acid in the different extracts from CSW. For CSW in

those conditions, the highest concentration for glucose, fructose, acetic acid, and for lactic acid was 10.36 g/L, 11.08 g/L, 0.03 g/L and was 0.03 g/L, respectively (as shown in Tables-2). As described earlier, the biosynthesis of cellulose is a multi-step reaction involving individual enzymes, catalytic complexes, and regulatory proteins. It contains four key enzymatic steps when glucose is used as carbon source (Figure-3). Bacteria cellulose production by *A.xylinum* proceeds mainly through glucose phosphate UDPglucose (UDPGlc) pathway. UGPase is thought to play an important role in cellulose synthesis since it is approximately 100 times more active in cellulose producers than that of noncellulose producing bacteria [9, 12]. When disaccharides, such as sucrose and maltose, are used as carbon source for cellulose-producing bacteria, the biosynthesis of BC starts with the hydrolysis of disaccharides into monosaccharides, such as glucose and fructose.

4.2 Cultivation of bacterial cellulose

Thirteen sets of experiments were conducted as described previously in the method section. Results are displayed in Table-3. As can be seen in the table, the best condition which maximum yield of bacterial cellulose (1.14 g) and the best of COD treatment (71.2%) can be carbon source (COD ratio) 11, 971 mg/L, 5 ml of *A.xylinum* added, and temperature 40 °C. These results are in good agreement with RSM results in which higher carbon source will result in higher yield (Equation 2) and the best of COD treatment (Equation 3). The worst condition yield of bacterial cellulose (0.08 g) was carbon source (COD ratio) 5,997 mg/L, 3 ml of *A.xylinum* added, and temperature 20 °C. From these results, bacterial cellulose from the best condition was selected to perform the chemical and physical properties as described above. The optimum conditions for yield of bacterial cellulose and COD treatment were determined by means of the BBD under RSM. The results are displayed in Table-3 could be expressed using the following equation:

$$Y = 0.512 + 0.385X_1 + 0.047X_2 + 0.043X_3 - 0.0457X_{12} + 0.055X_{22} + 0.022X_{32} + 0.038X_1X_2 + 0.031X_1X_3 + 0.009X_2X_3 \quad (2)$$

in which :
 Y = Yield (g)
 X_1 = Carbon source (COD ratio)
 X_2 = *A. xylinum*, and
 X_3 = Temperature

$$Y = 5255.65 + 372.78X_1 - 78.91X_2 - 78.91X_3 - 1769.78X_{12} - 79.78X_{22} + 400.22X_{32} - 134.44X_1X_2 + 25.56X_1X_3 - 217.83X_2X_3 \quad (3)$$

in which :
 Y = COD treatment (mg/L)
 X_1 = Carbon source (COD ratio)
 X_2 = *A. xylinum*, and
 X_3 = Temperature



Table-2. Composition of fermentation media used in this study.

| Before | | | After | | |
|--------|---------------|---------------|--------|-------------------|---------------|
| Run | Sucrose (g/L) | Average (g/L) | | Glucose (g/L) | Average (g/L) |
| CSW(1) | 80.36 | 80.43 | | 10.44 | 10.36 |
| CSW(2) | 80.50 | | | 10.28 | |
| | | | | Fructose (g/L) | Average (g/L) |
| | | | CSW(1) | 11.06 | 11.08 |
| | | | CSW(2) | 11.10 | |
| | | | | Lactic acid (g/L) | Average (g/L) |
| | | | CSW(1) | 0.03 | 0.03 |
| | | | CSW(2) | 0.03 | |
| | | | | Acetic acid (g/L) | Average (g/L) |
| | | | CSW(1) | 0.03 | 0.03 |
| | | | CSW(2) | 0.02 | |

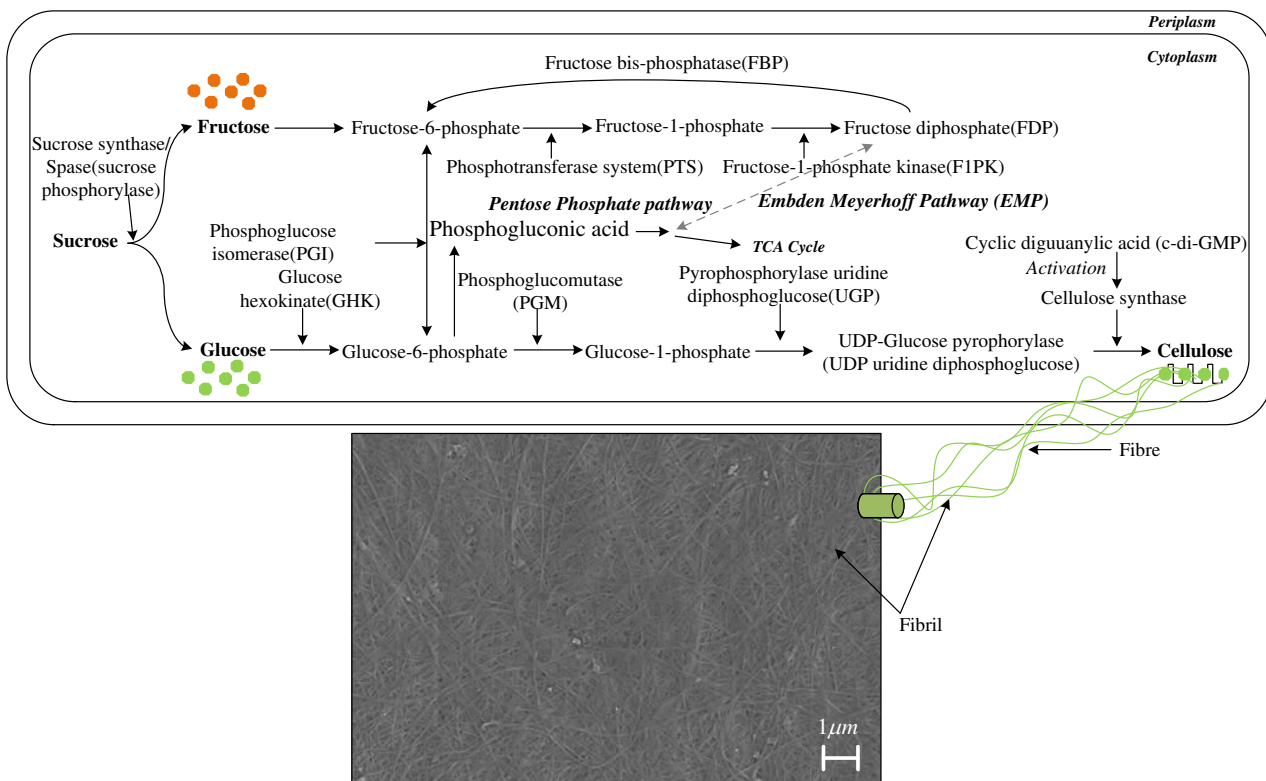


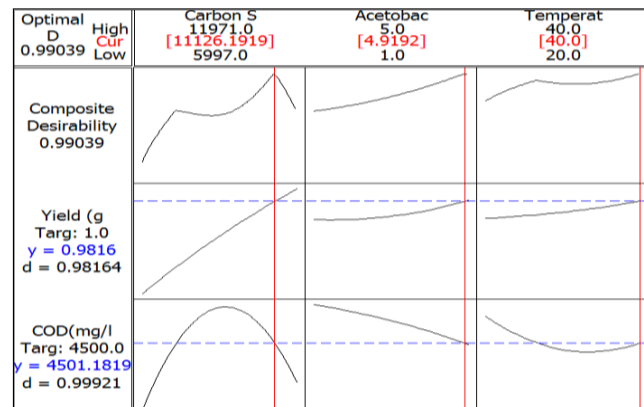
Figure-3. A schematic showing the major metabolic pathways of *Acetobacter xylinum* and the assembly of cellulose molecules into nano fibrils.

**Table-3.** Yield of bacterial cellulose and COD treatment from each set of experiment.

| Run | Carbon Source (COD ratio), mg/L | <i>A. xylinum</i> , mL | Temperature (°C) | COD _(treatment) (mg/L) | COD treatment (%) | Dried BC weight (g) |
|-----|---------------------------------|------------------------|------------------|-----------------------------------|-------------------|---------------------|
| 1 | 11,971 | 3 | 40 | 4480 | 62.6 | 0.93 |
| 2 | 8,996 | 5 | 40 | 5440 | 39.5 | 0.62 |
| 3 | 5,997 | 5 | 30 | 3200 | 46.6 | 0.13 |
| 4 | 11,971 | 5 | 30 | 3520 | 70.6 | 0.98 |
| 5 | 8,996 | 1 | 40 | 5760 | 36.0 | 0.58 |
| 6 | 11,971 | 1 | 30 | 3840 | 67.9 | 0.82 |
| 7 | 11,971 | 3 | 20 | 4480 | 62.6 | 0.78 |
| 8 | 5,997 | 3 | 20 | 3520 | 41.3 | 0.08 |
| 9 | 8,996 | 3 | 30 | 5120 | 43.1 | 0.55 |
| 10 | 8,996 | 5 | 20 | 5760 | 36.0 | 0.60 |
| 11 | 5,997 | 5 | 40 | 3140 | 47.6 | 0.22 |
| 12 | 5,997 | 3 | 40 | 3200 | 46.6 | 0.12 |
| 13 | 11,971 | 5 | 40 | 3450 | 71.2 | 1.14 |
| 14 | 8,996 | 1 | 20 | 5480 | 39.1 | 0.52 |
| 15 | 5,997 | 1 | 30 | 3200 | 46.6 | 0.11 |

4.3 Optimization curve

Response optimization helps identify the optimal factors that will give rise to an optimal response [14]. Here, the three factors were evaluated in order to get the values that will give the best condition which maximum yield of bacterial cellulose and COD treatment from the BBD model having an carbon source (COD ratio) 11, 971 mg/L. A target value for the yield of bacterial cellulose and COD treatment were set at 1 g and 4500 mg/L, respectively. The model predicted a 0.9816 g of yield of bacterial cellulose and 4501.18 mg/L of COD treatment with a composite desirability score of 0.98164 and 0.99921 respectively, as shown in Figure-4. To achieve such an excellent yield of bacterial cellulose and COD treatment, carbon source (COD ratio) 11,126.19 mg/L, 4.92 ml of *A. xylinum* added, and temperature 40 °C. Thus, a 0.9816 g of yield of bacterial cellulose and 4501.18 mg/L of COD treatment is guaranteed under the optimized conditions.

**Figure-4.** Process optimization curve for the yield of bacterial cellulose and COD treatment.

4.4 Characterization of BC and CANF

4.4.1 Structural analysis

Semi-acetylation of BC is considered to change its shape with the change of crystal structure of cellulose. Scanning electron microscope (SEM) images of BC and CANF are displayed in Figure-5a and 5b. As seen in the figure, CANF synthesized in this study was approximately 30-100 nm. All nanofibers of dried CANF sheets existed separately without coagulation, since the surface tension was reduced by the replacement of water with organic solvent acetic acid, toluene, perchloric acid and NaOH. As a result, CANF was obtained by the semi-acetylation method. Comparing images of figure 5a and 5b reveals that the reaction proceeds from the surface to the core of semicrystalline nanofibers, and the dimensions and crystal structure of the nanofibers were changed with the increase



of acetyl CANF. These changes affected various physical properties of the BC nanocomposites [15].

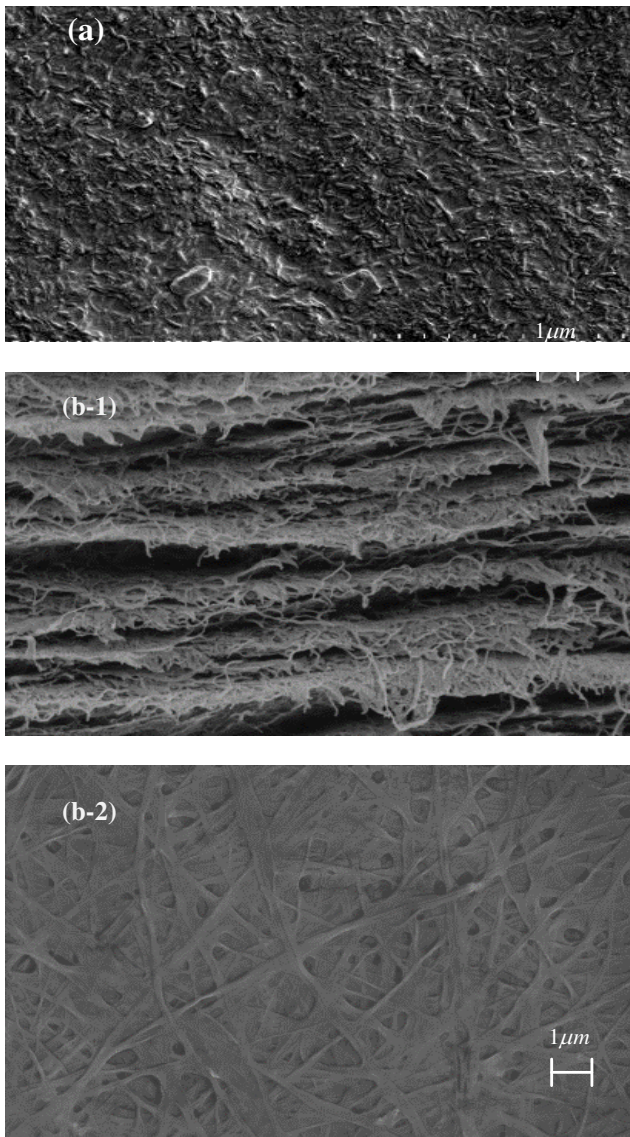


Figure-5. (a) SEM analysis of BC at 20,000x, (b-1, 2) SEM analysis of CANF at 20,000x

4.5 Tensile strength analysis

Table-4. Tensile strength of bacterial cellulose.

| No. | Young's modulus (Mpa) | | Tensile strength (Mpa) | |
|---------|-----------------------|--------|------------------------|-------|
| | BC [9] | CANF | BC [9] | CANF |
| 1 | 387.87 | 385.41 | 46.96 | 87.01 |
| 2 | 416.08 | 451.46 | 40.21 | 98.80 |
| 3 | 406.99 | 451.21 | 36.20 | 86.32 |
| Average | 403.65 | 429.36 | 41.13 | 90.71 |
| SD | 11.76 | 31.08 | 4.44 | 5.73 |

As listed in Table-4, average tensile strength of CANF and BC were 90.71 and 41.13 MPa, respectively. Comparison analysis with tensile strength of polycarbonate (62.01 MPa) reveals that CANF is strong as polycarbonate. This result also confirmed the FT-IR method of ethyl group from chemical structure analysis (described below), but BC is not as strong as polycarbonate [9].

4.6 FTIR spectra analysis

Functional group of chemical structure of BC and CANF was analyzed using ATR-FTIR; result was illustrated in Figure-6. From the figure, result indicated that chemical structure found from CANF were hydroxyl -OH (3343 cm^{-1}), -CH (1642 cm^{-1}) as show the hemicelluloses, and ethyl -CH₂ (1427 cm^{-1}) as show the celluloses, as shown in Table-5. Comparing chemical structure of BC to that of traditional CANF that the similar result can be observed with hydroxyl -OH, -CH, and ethyl -CH₂ [9], but BC is not as strong as CANF as listed in Table-4. Comparing chemical structure of BC and CANF to that of traditional plastic synthesized from petrochemical suggested that the similar result can be observed with the exception of methyl group (CH₃). Methyl group which can be found in plastic synthesized from petrochemical is responsible for the strength of plastic. Thus, CANF, synthesized in this study, is as strong as petrochemical plastic, because ethyl group (CH₂) [16, 17].

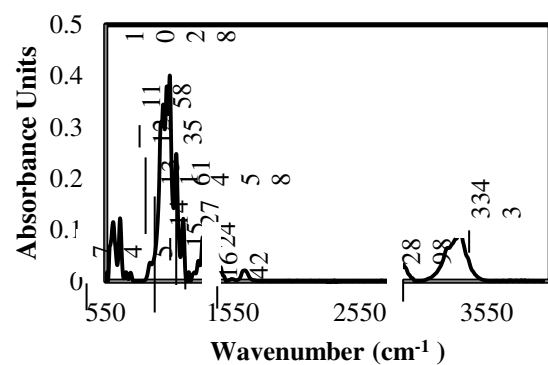


Figure-6. Spectra functional group chemical structure of bacterial cellulose in the range of 550-4000 cm^{-1} .

Table-5. Absorption wavenumber between the real and synthesized IR spectra of amorphous CANF.

| Wave number, cm^{-1} | Band assignment |
|-------------------------------|--|
| 3343 | O-H stretching (hydrogen-bonded) |
| 2898 | C-H stretching vibration in methyl and methylene groups |
| 1642 | Carbonyl stretching vibration in free aldehyde present in hemicelluloses |
| 1524 | C=C stretching vibration in aromatic structure |



| | |
|------|--|
| 1458 | C-H deformations; asymmetric bending vibration of -CH ₂ -groups |
| 1427 | CH ₂ bending vibrations related to the structure of cellulose |
| 1361 | CH deformation vibration; O-H bending vibrations in phenols |
| 1235 | C-O of guaiacyl unit |
| 1158 | Asymmetric bridge stretching vibration of C-O-C group in the structure of cellulose |
| 1028 | Symmetrical C-O stretching |
| 745 | Glucose ring stretching, C ₁ -H deformation; C-H stretching out of plane of aromatic ring |

4.7. Glasstransition temperature (T_g) analysis

The TGA curve of CANF showed a typical decomposition curve of pure compound where only one step of decomposition was observed [17, 18]. Thus confirming the purity of the polymer extracted from CSW. Since the analysis was performed under nitrogen atmosphere, no oxidation occurred. In this inert condition, sequence of reactions occurs as cellulose being heated. The first reaction is dehydration of cellulose, an endothermic process known as dehydrocellulose [17, 19, 20]. After that, depolymerization reaction took place and yielded levoglucosan (1, 6-anhydro-β-D-glucopyranose) as an essential intermediate. Finally, the TGA curve of CANF showed a typical decomposition curve of pure compound a cellulose, lignin and hemicellulose as shown in Figure-7.

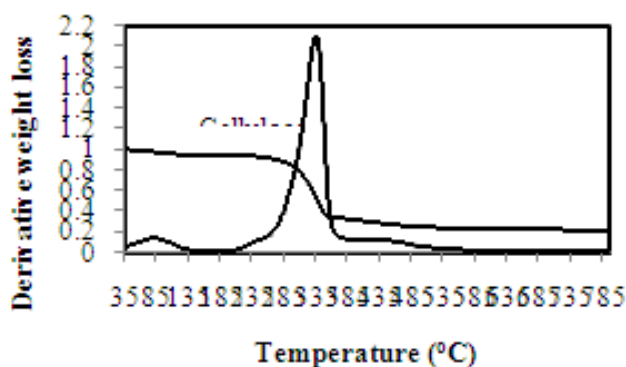


Figure-7. TGA curves in nitrogen atmosphere at a heating rate of 20 °C/min.

5. CONCLUSIONS

Base on the results of this study, bacterial cellulose can be synthesized from a cultivation of CSW using *A.xylinum*. The best conditions for cultivation to obtain the maximum yield (1.14 g) and COD treatment (71.2 %) were carbon source (COD ratio) equalled 11, 971 mg/L, 5 ml of *A.xylinum* added, and 40 °C of incubating temperature. Scanning electron microscope (SEM) images of CANF synthesized in the study was approximately 30-

100 nm. The cellulose extracted from CSW met the specifications of pure cellulose, as proven by FTIR, thermal properties and solubility studies. The FTIR spectra of CANF from CSW showed distinguished peaks at 3343 cm⁻¹, 2898 cm⁻¹, 1458 cm⁻¹, 1427 cm⁻¹, 1158 cm⁻¹ and 1028 cm⁻¹ which correspond to O-H stretching, C-H stretching, C-H bending, CH₂ bending, C-O-C stretching and C-O stretching, respectively. UTM analysis indicated that the CANF synthesized in this study has better properties that those of BC. While the DTG showed maximum weight loss at 430°C, this value was within the range of observed cellulose degradation peaks reported in the literature. The solubility of CANF in only one step of decomposition was confirms the purity of the cellulose. Based on the above research, CANF indicated good potential of the synthesized CANF to be further utilized as biofilm in VOCs treatment in air application in future.

ACKNOWLEDGEMENTS

This work was supported by Walailak University (Contract No. WU58610). This work was supported by Walailak University Fund (Contract No.19/2557) and this study was financially supported by Walalak University (Contract No. 08/2561).

REFERENCES

- [1] M. Z. H. Khan, M. Sultana, M. R. Al-Mamun and M.R. Hasan. 2016. Pyrolytic Waste Plastic Oil and Its Diesel Blend: Fuel Characterization. Journal of Environmental and Public Health. 1-6.
- [2] P. Chowdhury, T. Viraraghavan and A. Srinivasan. 2010. Biological treatment processes for fish processing wastewater: A review. Carbohydrate Polymers. 10: 439-449.
- [3] X. Zeng, D. P. Small and W. Wan. 2011. Statistical optimization of culture conditions for bacterial cellulose production by *Acetobacter xylinum* BPR 2001 from maple syrup. Carbohydrate Polymers. 85: 506-513.
- [4] D. Bingol. 2011. Removal of cadmium (II) from aqueous solutions using a central composite design, Fresenius Environmental Bulletin. 10: 2704-2709.
- [5] D. Das and N. Das. 2011. Response surface approach for the bisorption of Ag (I) by Macrofungus *Pleurotus platypus*. Clean - Soil, Air, Water. 2: 157-161.
- [6] P. Kaushik and A. Malik. 2011. Process optimization for efficient dye removal by *Aspergillus lentulus* FJ17299. Journal of Hazardous Materials 185: 837-843.



- [7] V. Ponnusami, V. Krithika, R. Madhuran and S. N. Srivastava. 2007. Biosorption of reactive dye using acid-treated rice husk: factorial design analysis. *Journal of Hazardous Materials*. 142: 397-403.
- [8] A. Fakhri. 2014. Application of response surface methodology to optimize the process variables for fluoride ion removal using maghemite nanoparticles. *Journal of Saudi Chemical Society*. 18: 340-347.
- [9] K. Sunun, K. Wipawee, S. Kowit and S. Wipada. 2014. Characteristics of bacterial cellulose production from agricultural wastes. *Advanced Materials Research*. 931-932: 693-697.
- [10] E. J. Vandamme, S. D. Baets, A. Vanbaelen, K. Joris and P.D. Wulf. 1998. Improved production of bacterial cellulose and its application potential. *Polymer Degradation and Stability*. 59: 93- 99.
- [11] K. Y. Benyounis, A. G. Olabi and M. S. J. Hashmi. 2015. Effect of laser welding parameters on the heat input and weld-bead profile. *Journal of Materials Processing Technology*. 164: 978-980.
- [12] L. Koon-Yang, B. Gizem, M. Athanasios and B. Alexander. 2014. More than meets the eye in bacterial cellulose: Biosynthesis, bioprocessing and applications in advanced fiber composites. *Macromolecular Bioscience*. 14: 10-32.
- [13] K. Suwannahong, W. Sanongraj, P. Noophan and S. Sirivithayapakorn. 2014. Improvement of TiO₂/LDPE composite films for photocatalytic oxidation of acetone. *Advanced Materials Research*. 931-931: 235-240.
- [14] I. D. Gaddafi, A. S. Tawfik and A. S. Abdullahi. 2016. Response surface methodology optimization of adsorptive desulfurization on nickel/activated carbon. *Chemical Engineering Journal*. 313: 993-1003.
- [15] S. Ifuku, M. Nogi, K. Abe, K. Handa, F. Nakatsubo and H. Yano. 2007. Surface modification of bacterial cellulose nanofibers for property enhancement of optically transparent composites: Dependence on acetyl-group DS. *Biomacromolecules Journal*. 8: 1973-1978.
- [16] M. Akerholm, B. Hinterstoisser and L. Salmen. 2004. Characterization of the crystalline structure of cellulose using static and dynamic FT-IR spectroscopy. *Carbohydrate Research*. 3: 569-578.
- [17] N. Halib, M. Cairul, I. M. Amin and I. Ahmad. 2012. Physicochemical properties and characterization of nata de coco from local food industries as a source of cellulose. *Journal Sains Malaysia*. 41(2): 205-211
- [18] C. Katepetch and R. Rujiravanit. 2011. Synthesis of magnetic nanoparticle into bacterial cellulose matrix by ammonia gas-enhancing in situ co-precipitation method. *Carbohydrate Polymers*. 86: 162-170.
- [19] M. Karim, N. B. Mohamed and B. Julien. 2013. Nanofibrillated cellulose surface modification: A review. *Journal of Materials Science*. 6: 1745-1766.
- [20] S. M. Santos, J. M. Carbajo and J. C. Villar. 2013. The effect of carbon and nitrogen sources on bacterial cellulose production and properties from *Gluconacetobacter sucrofermentans* CECT 7291 focused on its use in degraded paper restoration. *Bio Resources*. 8(3): 3630-3645.